

Variable-Bandwidth Optical Paths: Comparison Between Optical Code-Labeled Path and OCDM Path

Shaowei Huang, *Student Member, IEEE*, Ken-ichi Baba, Masayuki Murata, *Member, IEEE*, and Ken-ichi Kitayama, *Fellow, IEEE*

Abstract—In a conventional wavelength-routed network, the bandwidth of one wavelength is considered as the minimum granularity for a given connection request. Therefore, no multiple connection requests can be accepted by using a single wavelength simultaneously. This may cause inefficiency in the bandwidth utilization in some cases. In this paper, the focus is on the variable-bandwidth approach called an optical code (OC)-based path to improve this bandwidth utilization. The concept of OC-enabling paths is investigated, which shows its potential in resolving the above granularity problem inherent to the wavelength-routed network. First, two optical paths, called the OC-labeled and OC division multiplexing (OCDM) paths, are proposed. The former is based upon label switching and statistical multiplexing, while the latter is based upon OCDM. Next, OC-label and OCDM optical cross connects are described to support OC-labeled and OCDM paths, respectively. In this paper, a coherent time-spread OC is adopted. A two-state flow-fluid traffic model is addressed and regarded as the general analysis model. Finally, the performances between these proposed paths are qualified and compared, and numerical results show that the OC-labeled path outperforms the OCDM path under short burst duration time, whereas the OCDM path, provides higher flexibility than the OC-labeled path, owing to its independence of burst duration time.

Index Terms—Optical code division multiplexing (OCDM) optical cross connect (OXC), optical code division multiplexing (OCDM) path, optical code (OC)-labeled optical cross connect (OXC), optical code (OC)-labeled path, variable-bandwidth optical path.

I. INTRODUCTION

GENERALIZED multiprotocol label switching (GMPLS) [1] is going to play an important role in migrating MPLS-based control-plane techniques into the optical layer in IP-over-wavelength-division-multiplexing (WDM) networks. There are several degrees of data granularity described in [1]. Though packet-switched, time-division-multiplexed (TDM), wavelength-switched, and fiber-switched capable interfaces are regarded as the fundamental elements in GMPLS, the wavelength is still taken as the minimum granularity in optical-path establishment and provision in many studies.

Manuscript received March 24, 2005; revised January 3, 2006.

S. Huang and K. Kitayama are with the Graduate School of Engineering, Osaka University, Suita, Osaka 565-0871, Japan (e-mail: huangshw@ac.eie.eng.osaka-u.ac.jp; kitayama@comm.eng.osaka-u.ac.jp).

K. Baba is with Cybermedia Center, Osaka University, Ibaraki, Osaka 567-0047, Japan (e-mail: baba@cmc.osaka-u.ac.jp).

M. Murata is with the Graduate School of Information Science and Technology, Osaka University, Suita, Osaka 565-0871, Japan (e-mail: murata@ist.osaka-u.ac.jp).

Digital Object Identifier 10.1109/JLT.2006.872319

However, it is not always the case that one end-to-end connection requires the whole bandwidth of one wavelength, thus resulting in low bandwidth utilization. To improve the bandwidth utilization, the study of the TDM-based wavelength-routed network architecture has also been carried out, in which paths labeled with special time slot(s) are multiplexed in a single wavelength [2]. It has been proven to be suitable to multirate traffic with various numbers of assigned time slots. However, it lacks in flexibility as only a fixed number of time slots can be adopted in one wavelength, and in other words, all the multiple paths are multiplexed with a peak-rate multiplexing mechanism [8].

In this paper, we present a novel network architecture, called the optical code (OC)-based path network, to provide a variable-bandwidth optical path. Optical paths are of variable bandwidth, identified by OC sequences, and they are bundled into a single wavelength. Two approaches, called OC-labeled path and OC division multiplexing (OCDM) path, are studied. In the former, an OC label is attached to the head of a packet, while in the latter one, each bit in the packet is encoded by a specific OC. Both the OC label and OC (we call it OC identifier in our paper) can be recognized by the optical correlation in the optical domain. The combination of OC- and wavelength-based routing has been presented [3], but the architectural consideration is not included in the previous study. In this paper, we describe the optical cross-connect (OXC) architectures to support our proposed OC-labeled path and OCDM path in Section II.

A two-state flow-fluid traffic model, which can deal with different traffic patterns ranging from bursty to continuous bit stream [4], [8], is employed in the performance analysis of both OC-based paths. In the OC-labeled-path case, statistical multiplexing described in [4] is adopted instead of peak-rate multiplexing in [2], and the packet-loss probability (PLP) due to the buffer overflow is evaluated. In the OCDM-path case, multiple access interference (MAI) is considered as the main factor degrading network performance in our study. An approximate mathematical model taking MAI into account is proposed to qualify the performance with respect to packet-error probability. To achieve satisfactory performance in the OCDM system, coherent time-spread OC generation and recognition based upon superstructure fiber Bragg gratings (SSFBGs) [5]–[7], [27], [31] is introduced.

The remainder of this paper is organized as follows. Section II shows the basic concept of the OC-based path. In Section III, two OXC architectures are described to support packet switching for the OC-labeled and OCDM paths.

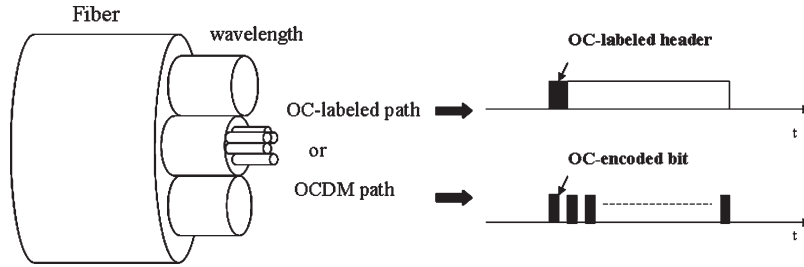


Fig. 1. Variable-bandwidth optical path in the conventional wavelength-based network.

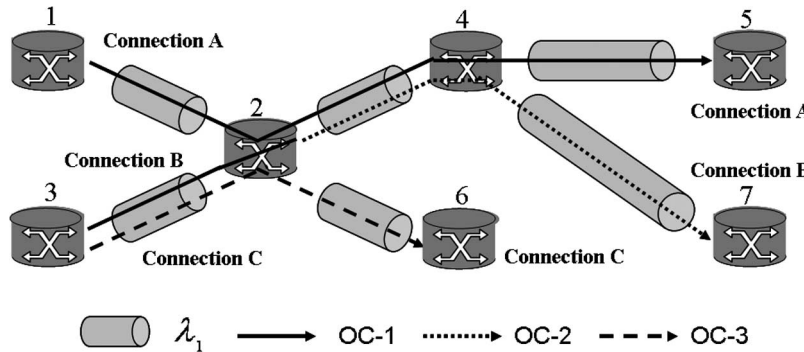


Fig. 2. OC-based routing and OC allocation scenario.

The approximate signal-to-noise ratio (SNR) of the gold code in such a coherent OCDM system is evaluated by a statistical approach. In Section IV, the traffic model, the statistical-multiplexing approach for the OC-labeled path, and the overlapped model for the OCDM path are described in detail. Section V shows the performance evaluation and comparisons between the OC-labeled and OCDM paths with different traffic characteristics and system properties. Finally, we summarize the findings and draw a brief conclusion.

II. CONCEPT OF THE OC-BASED PATH

The concept of variable-bandwidth optical paths originated from the bandwidth partition in ATM networks [8]. The OC-based path can provide the existing switching network architecture consisting of fiber switching, waveband switching, and wavelength switching with a finer and more flexible granularity in the bandwidth. It has a capability to adjust the number of optical paths that can be multiplexed in a single wavelength with different traffic characteristics and different levels of quality of service (QoS, e.g., PLP). The hierarchical model is illustrated in Fig. 1. One will be able to see that the combination of the OC-based path with the conventional wavelength-based path makes the bandwidth utilization of a single wavelength more efficient and flexible, which may lead to another novel approach in grouping optical paths.

A. Basic Concept of the OC-Based Path

In our proposed network architecture, multiple OC-based paths are multiplexed in a single wavelength using either an OC label or the OC itself. The OC can be incorporated for one of the optical labels into GMPLS. The combination of wavelength and OC leads to a two-dimensional routing problem, in which both the wavelength and the OC are considered as

available resources. Here, we first classify the OC-based path network architecture into four categories as follows, depending on the availability of wavelength/OC conversion in the OXC:

- 1) nonwavelength conversion and non-OC conversion;
- 2) nonwavelength conversion, but OC conversion;
- 3) wavelength conversion, but non-OC conversion;
- 4) wavelength conversion and OC conversion.

It is apparent that the first one is the simplest but lacks in flexibility when conflict occurs at the output port, which may result in high blocking probability in some cases, while the last one outperforms all the others with its highest flexibility in reducing blocking probability or PLP but would result in system complexity and high cost. With the current state of the art, wavelength conversion is still immature. In addition to this, the multiplexing effect that OC-based paths play to improve bandwidth utilization is the main objective in our paper; therefore, we concentrate on the second kind, where OC conversion, and not wavelength conversion, is adopted in the OXC to obtain the tradeoff in performance and system stability. As compared with wavelength conversion, OC conversion can be achieved at high speed and provide a relatively stable conversion performance, as described in [3]. The case with wavelength conversion and OC conversion will be studied in the future.

Fig. 2 illustrates the OC-based routing and OC allocation scenario. For simplicity, we assume that different optical paths are multiplexed in one wavelength by using OC identifiers. Without loss of generality, each connection only occupies one OC in each link. Here, connection A's traffic is routed from node 1 to node 5; connection B's traffic is routed from node 3 to node 7; and connection C's traffic is routed from node 3 to node 6. As shown in the routing table stored in node 2 in Table I, the traffic of connections A and C, identified by OC-1 and OC-3, respectively, are routed through node 2 without any conversion, while that to connection B, which is denoted as

TABLE I
CONCEPT OF OC-BASED ROUTING

Connection Session	Incoming		Outgoing	
	Port No.	OC	Port No.	OC
A(1, 5)	1	1	1	1
B(3, 7)	2	1	1	2
C(3, 6)	2	3	2	3

OC-1, is converted to OC-2 through OC conversion to avoid conflict with connection A.

B. Properties of the OC-Labeled and OCDM Paths

In Section II-A, we described our OC-based path network architecture. To multiplex multiple optical paths in a single wavelength, we propose two approaches, called OC-labeled and OCDM paths.

Deriving from an analogy of a virtual channel (VC) in ATM networks [8], in the OC-labeled path, an OC label is encapsulated in the header of the data payload, and packets with the same label, which should be routed on the same optical path, are considered to belong to a single connection. This is also similar to the definition of a label-switched path (LSP) in GMPLS [1], except that label recognition and swapping are performed with the approaches presented in [3], [9], and [10]. We will explain the related issues in detail in Section III. The OC-labeled path employs statistical multiplexing for the paths sharing the bandwidth of a single wavelength. Based upon the equivalent-capacity theory [4], it is possible for us to estimate the bandwidth required by each connection in terms of PLP.

On the other hand, in the OCDM-path case, each bit in the payload is encoded by an OC instead of a header [3]. Then, optical paths encoded by different codes can overlap with each other. In our proposed OXC in Section III, OCDM paths are discriminated by the decoders, and each payload is forwarded to a specific output port according to its own OC. The performance of an OCDM system is affected by additive noises as well as the MAI noise, which is regarded as the main factor of performance degradation in the OCDM path. The more active users are accommodated in a network, the poorer the attained performance will be [23], [24]. OCDMA can be classified into incoherent OCDMA [25], [26], where encoding is based upon optical intensity, and coherent OCDMA, where encoding is based upon amplitude (with phase) [3], [7], [27], [31]. A variety of OC sequences [32]–[35] are available, for example, prime code, optical orthogonal code (OOC), and gold code, etc. As high-performance OC generation/recognition based upon an SSFGB with gold code has been demonstrated successfully recently [7], we also adopt such a system in our OCDM path, which will be described in Section III in detail.

III. ARCHITECTURES OF OXC

A. OC-Label OXC

The design of the OC-Label OXC is based upon the large body of architectural studies in the literature of optical packet switching (OPS) [10]–[20]. According to the latest research,

the main functions of an optical packet switch include routing, switching, as a contention-resolution mechanism, and as a control unit. To the label-switched network, routing and switching perform label recognition/swapping and switch packets to the desired output ports. In [10], an in-band labeling technology based upon a coherent OC was presented to support label recognition and swapping and was demonstrated successfully by experimentation, where a high throughput of 100 Tb/s has been achieved through OC correlation. Such architecture is applied to our OC-label OXC and will be explained later in this section. The contention-resolution mechanism is used to resolve a situation whenever two packets are routed to the same output port simultaneously. To achieve this, optical buffers based on a fiber delay line (FDL) and wavelength conversion have been introduced [10]–[14], [15]–[19]. As described above in Section II, no wavelength conversion is adopted in our switch; we use FDL for contention resolution instead of a wavelength converter. The control unit ensures that the switch maintains the information of local ports, which takes responsibility for the switch configuration and forwarding decision.

Switches using FDL for contention resolution can be classified into input buffered and output buffered, where the former adopts the FDL ahead of the switching elements [11], and the latter adopts the FDL after them [11]–[13], [17], [19], [20]. However, most of them only considered the single-wavelength case. In [17], [20], and [21], switches called WDM version optical packet switches are described, which are capable of handling WDM input/output ports. In WDM version switches, all the input wavelength channels are demultiplexed to n (n is referred to as the number of wavelength channels per input) parallel switching planes, and wavelength conversion is enabled by a tunable wavelength converter (TWC) in each switching plane. Additionally, the switch architecture of each switching plane can be similar to that of the traditional one. Because no wavelength conversion is considered in our above assumption in Section II, we modify the above WDM version switches, in conjunction with that in [10], to each switching plane to form the OC-label OXC.

As illustrated in Fig. 3, it consists of three units: wavelength demultiplexer/multiplexer, switch plane, and scheduler. This switch plane plays a key role in this OXC. It consists of four elements: an OC-label processor (for label recognizing), an OC-label swapper (for label swapping), an optical switch fabric, and an FDL for the buffer. Note that the number of switching planes is equal to that of incoming wavelengths demultiplexed at the input port. The scheduler is responsible for controlling the buffer by updating and providing the information of the status of the OC-label swapper, the optical switch fabric, and the FDL, as well as maintaining the routing table. After receiving the signals from the OC-label processor, the scheduler makes a decision to set up the OC-label swapper and optical switch fabric for packet forwarding.

It is apparent that contention will occur at the output port if more than two packets from different input ports are switched to the same output port. To avoid this contention, buffer management based upon FDL is a key issue. Based upon the information provided by the header and the status of the buffer, the scheduler makes a decision for selecting both an appropriate

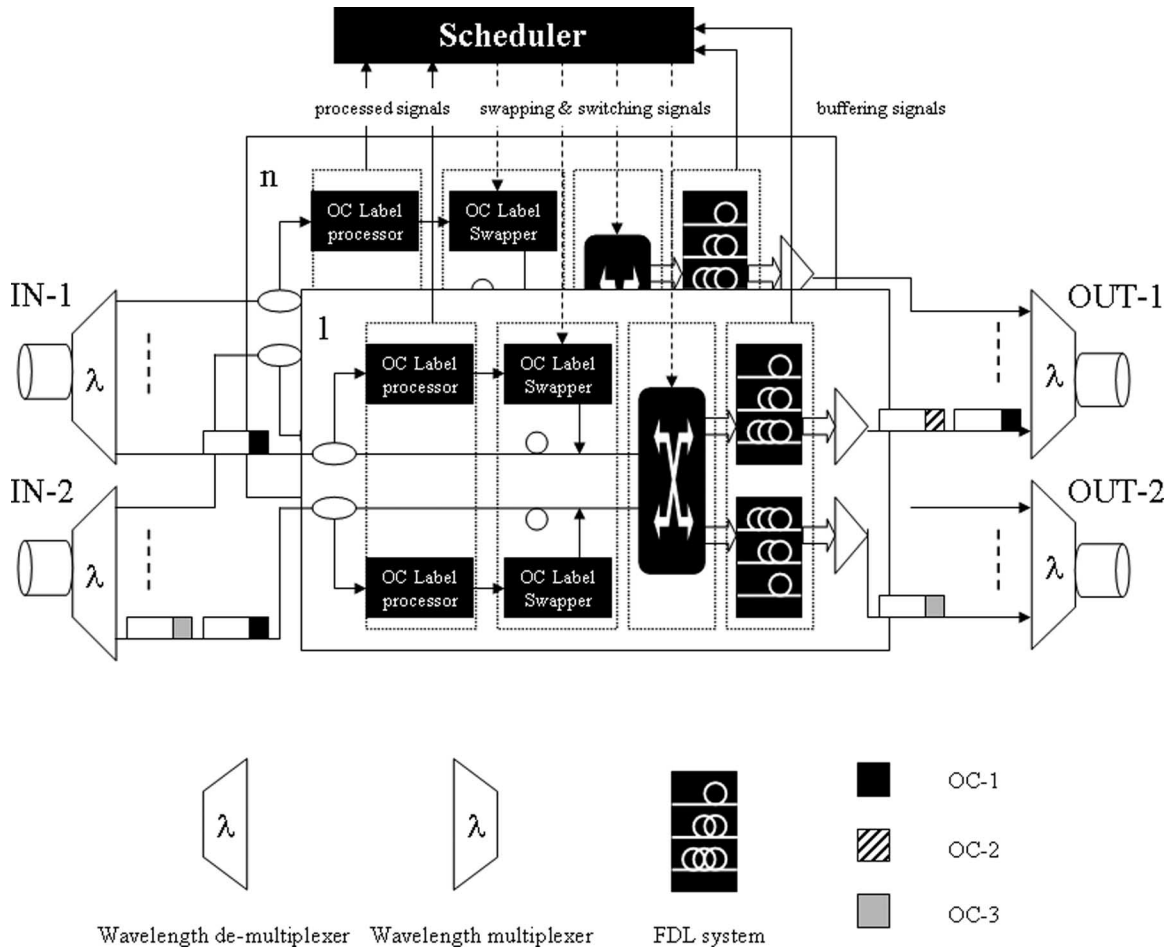


Fig. 3. Architecture of OC-label OXC with a 2 x 2 port size.

FDL entry and an appropriate OC label for swapping. Buffer management is referred to the bottleneck to balance the tradeoff between service quality (e.g., PLP, delay, etc.) and switch throughput. For this purpose, an optimized buffer-management algorithm is desired [22].

B. OCDM OXC

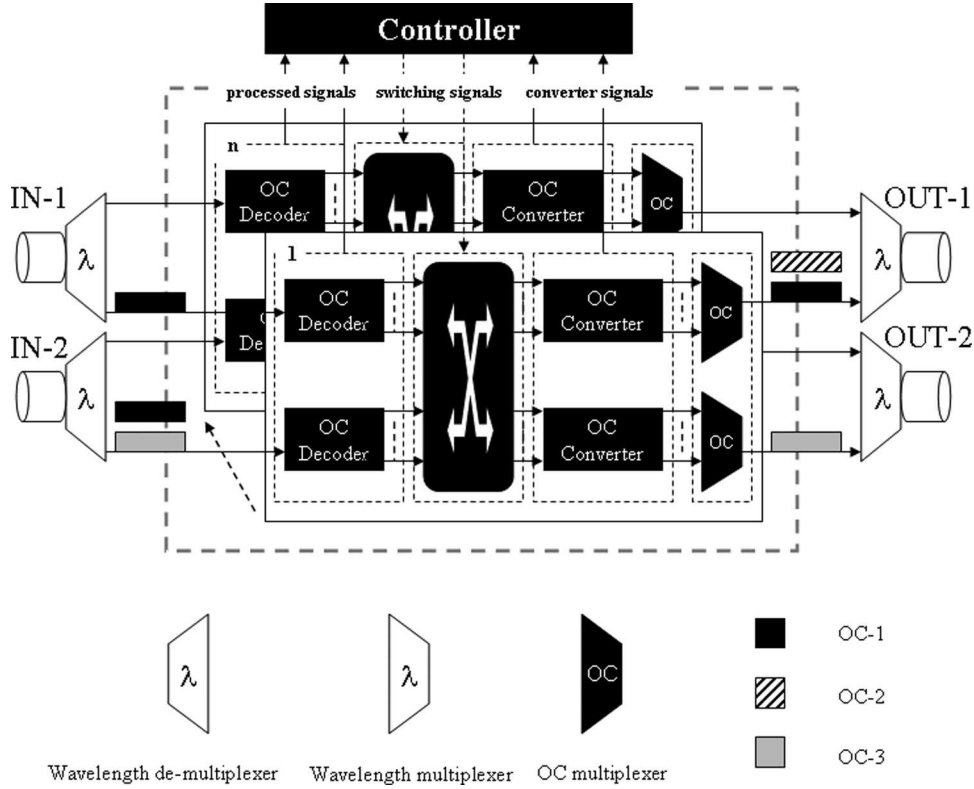
Fig. 4 illustrates the architecture of a 2 x 2 OCDM OXC. The composition is similar to that of an OC-label OXC: wavelength demultiplexer/multiplexer, switch plane, and controller. The difference from the OC-label OXC is the switch-plane architecture. In the OCDM OXC, no buffer mechanism is needed to adopt at the output for contention resolution because channels encoded by distinct code sequences can overlap each other in the time domain, which works in the tell-and-go mode. This is quite similar to the wavelength-conversion buffer system. The controller only takes responsibility for the setup of the central optical switch component for 1) forwarding the packet to a specific output port and 2) assigning a packet with a new OC to avoid contention at the output port.

Owing to the advantage of asynchronous access property in OCDMA [23], [24], asynchronous traffic can be handled in our OCDM OXC, which is regarded as the great benefit of simplifying the algorithm design for contention resolution compared with the complex buffer-management mechanism

in the FDL-buffered switch. The main procedures of packet switching mainly involves four steps.

- Step 1) Multiple channels are first demultiplexed before entering the switching plane.
- Step 2) OC recognition (path discrimination) is performed in the OC decoder array, which consists of m (m is the number of OCDM channels per wavelength) decoders.
- Step 3) The controller sets up the optical switch fabric according to the processed OC of the incoming packet. In fact, because the converter is a passive optical waveguide device, OC conversion will be carried out in the switch-fabric setup consequently. As described above, contention at the output port can be resolved with some algorithms.
- Step 4) Signals passing through OC converters are multiplexed by the OC multiplexer and are prepared for transmission to the next hop.

Hence, the advantages of the OCDM OXC can be summarized as follows: 1) Nonbuffer operation leads to a simple switch-architecture design and controlling mechanism; 2) asynchronous traffic is supported, which is more suitable in the practical case; and 3) all-optical processing can be possible, which is of great benefit to achieve high throughput.


 Fig. 4. Architecture of OCDM OXC with a 2×2 port size.

C. Optical Processing (Encoding and Decoding)

In the incoherent time-spreading OCDMA, coding is based upon optical power, corresponding to light “ON” or light “OFF.” This leads to a limited code space and poor correlation property [25], [26]. Therefore, it does not seem appropriate to establish a high-performance OCDM path in our study. In contrast, a coherent OCDMA outperforms the incoherent scheme, as coding is based upon optical amplitude, where each chip in a code sequence can have a phase “0” or “ π ” with a binary-phase-shift-keying (BPSK) scheme [3], [9], [10], [21]. Recently, 511-chip-long OC generation and recognition using an SSFBG have been achieved [7].

Our choice is the above coherent OC. Fig. 5(a) illustrates the working principle of the SSFBG with a slowly varying refractive-index modulation profile imposed along its length and phase shifts inserted between segments. With this device, a series of coherent short optical pulses whose phases are determined by the pattern of the phase shifts in the SSFBG will be generated.

As an example, Fig. 5(b) illustrates a seven-chip OC generation (encoding) with a BPSK scheme by employing the SSFBG [7]. Among the generated optical pulses, the white ones hold a phase of “0,” while the gray ones “ π .” T_{chip} denotes the chip duration time, n denotes the refractive index of the optical fiber, and c denotes the velocity of light in a vacuum. The L_{chip} of one segment can be defined as $L_{\text{chip}} = T_{\text{chip}}/(2nc)$ [7].

In Fig. 5(c), decoding processes are carried out with the same device. As the decoder in Fig. 5(c) matches the encoder in Fig. 5(b), a peak pulse can be attained. Here, the data-rate detection is employed instead of chip-rate detection, where an optical

thresholding technique can be employed to improve the performance in a practical OCDMA system [28]–[31], [36]. That is, using supercontinuum (SC) generation in a normal dispersion-flattened fiber (DFF) before the photodetector, as mentioned in [31], is adopted in our OCDM path. With the power transfer function of the SC-based optical thresholder (shown in [31]), MAI noise less than 0.5 mW will become very small (nearly 0) after passing through the optical thresholder. We use the gold code in our OCDM path for encoding. Though the beat noise is another dominant noise in a coherent OCDMA system [35], we only take MAI noise into account to check the feasibility of the OCDM path. By employing the optical thresholder, the SNR for 31-, 127-, 255-, 511-, and 1023-chip gold codes are analyzed, which correspond to the ratio of normalized peak intensity of the autocorrelation to the normalized variance of the interfering signal. Here, the normalized variance of the interfering signal is an assemble average. The variance values are shown in Table II. Let N denote code length.

Letting K denote the number of active users, the SNR can be given by

$$\text{SNR}(N, K) = \frac{1}{\sigma^2(N) \times (K - 1)}. \quad (1)$$

The bit error rate (BER) can be expressed as

$$\text{BER} = \Pr(b = 0) \cdot \Pr(Z > \text{Th} | b = 0) + \Pr(b = 1) \cdot \Pr(Z < \text{Th} | b = 1) \quad (2)$$

where Th is defined as the normalized threshold for the decision. The terms $\Pr(b = 0)$ and $\Pr(b = 1)$ are the probabilities

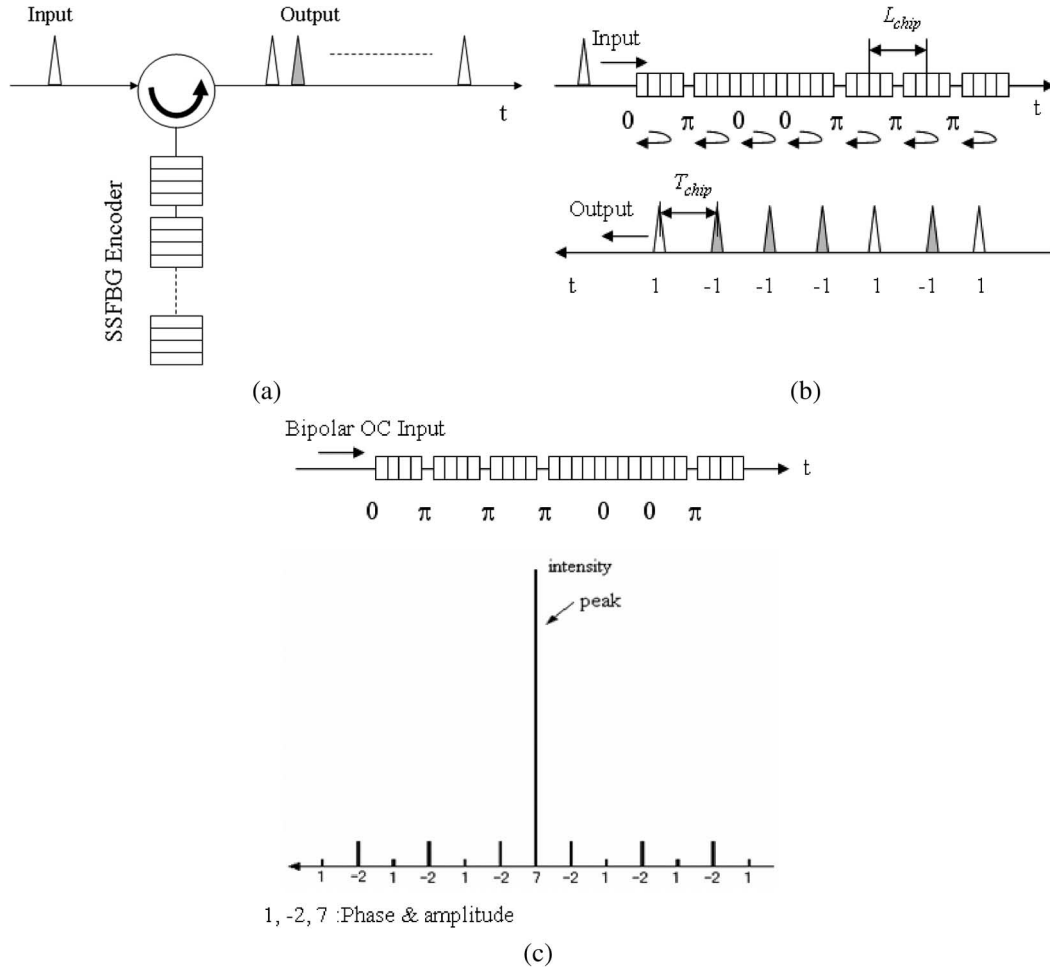


Fig. 5. OC processing. (a) OC encoder based upon SSFBG. (b) Seven-chip bipolar OC encoding with SSFBG. (c) Autocorrelation of seven-chip bipolar OC with SSFBG (decoding).

TABLE II
NORMALIZED VARIANCE FOR THE GOLD CODE

Code Length N	Variance $\sigma^2(N)$
31	1.08×10^{-2}
127	3.8×10^{-3}
255	2.07×10^{-3}
511	1.6×10^{-3}
1023	0.86×10^{-3}

for bit b “0” and “1,” respectively, and $\Pr(b = 0) = \Pr(b = 1) = 1/2$. The second term of (2) can be considered as zero for $0 < Th \leq 1$ because the output signal with a normalized autocorrelation peak is always not smaller than 1. Hence, (2) can be simplified as

$$\begin{aligned} \text{BER}(N, K) &= \frac{1}{2} \Pr(Z > Th | b = 0) \\ &= \frac{1}{2} \text{erfc} \left(\frac{Th}{\sqrt{2}} \cdot \sqrt{\text{SNR}(N, K)} \right). \end{aligned} \quad (3)$$

From (3), we can see that the BER is influenced by Th , even with the same number of active users. In [25], a variable optimum optical threshold Th can help to improve bit error performance. However, for simplicity and considering that it is

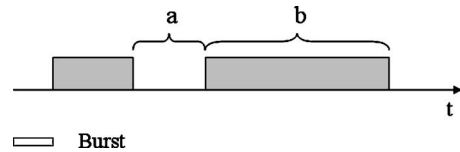


Fig. 6. Two-state flow-fluid traffic model.

not the main point in our paper, fixed threshold detection is employed, which is set to the normalized autocorrelation peak “1.”

IV. TRAFFIC MODELING

A traffic model, which is called a two-state fluid-flow model [8], is used in this study. As shown in Fig. 6, there are four parameters, namely, peak rate R_{peak} , a and b (periods during which the source is idle or active, respectively), and the fraction of time that the source is active, which is defined to be source utilization ρ . Therefore, the connection behavior can be characterized by the metric (R_{peak}, b, ρ) [4].

A. Equivalent-Capacity Model for the OC-Labeled Path

With the above traffic model, each OC-labeled path can be regarded as a two-state Markov source. Therefore, in the

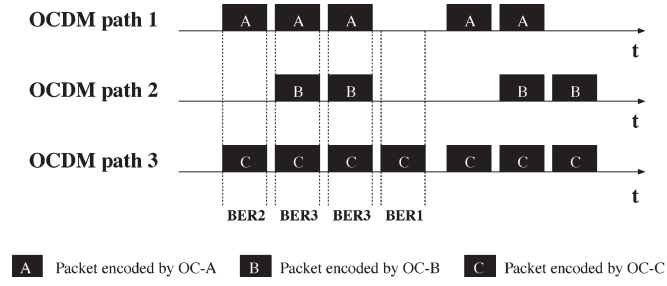


Fig. 7. Overlapped traffic model.

case of multiple OC-labeled paths accommodated in a single wavelength, the total bandwidth demanded by them can be given by [4]

$$\hat{C}(M) = \sum_{i=1}^M \hat{c}_i \quad (4)$$

where M is the number of multiple OC-labeled paths accommodated, and \hat{c}_i is the equivalent bandwidth demanded by i th OC-labeled path. \hat{c}_i is determined by the metric $(R_{\text{peak}}, b, \rho)$ described above and a desired QoS qualified by PLP. Let ε denote PLP, and $\alpha = \ln(1/\varepsilon)$. Let B denote buffer size, which can be given as in (5), shown at the bottom of the page [4]. Given OC-labeled paths with identical property, let $C_{\text{wavelength}}$ denote the total capacity of a wavelength, and let $c((R_{\text{peak}}, b, \rho), \varepsilon)$ denote the demanded capacity with metric $(R_{\text{peak}}, b, \rho)$ and PLP ε , which can be attained with the above formula. Hence, the number of OC-labeled paths accommodated in a single wavelength can be given as

$$M_{\text{max}} = \frac{C_{\text{wavelength}}}{c((R_{\text{peak}}, b, \rho), \varepsilon)}. \quad (6)$$

B. Overlapped Model for the OCDM Path

A mathematical model for evaluating the OCDM path is proposed by taking MAI into account as below. As shown in Fig. 7, three OCDM paths are multiplexed in a single wavelength.

In Fig. 7, the packets belonging to different OCDM paths are synchronized and are aligned in the time domain. We consider it to be the worst case, which gives the upper bound for PLP with the same given source utilization ρ , and leads to a simple analysis of the PLP calculation. If we assume that an error occurring in a single bit of the packet results in a whole packet error, the following formula can be used to interpret BER to PLP:

$$P_L(N, i) = 1 - (1 - \text{BER}(N, i))^{\text{plength}} \quad (7)$$

where i is the number of active users or, in other words, the number of overlapped packets at epoch $t(i)$, N is the code

 TABLE III
 NOTATIONS IN NUMERICAL CALCULATION

Symbol	Definition	Value
R_{peak}	Peak rate	200Mbps, 1Gbps, etc
ρ	Source utilization	0.3, 0.5, 1.0, etc.
b	Burst duration time	0.001s, 0.0001s, etc
B	Buffer size	50/100 packets, etc.
L	Code length	127, 511, etc.
PLP	Packet loss probability	10^{-3} , 10^{-8} , etc.
C	Capacity of one wavelength	10 Gbps
plength	Packet length	1500 bytes

Note that: in QC labeled path, peak rate is referred to as the average physical transmission bit rate; while in OCDM path, peak rate is referred to as the absolute physical transmission bit rate.

length, and plength is the packet length. Here, $\text{BER}(N, i)$ is given by (3). As shown in Fig. 7, $\text{BER}_1 < \text{BER}_2 < \text{BER}_3$ can be obtained easily. With the above model, the average PLP of the OCDM system can be given as

$$\text{PLP}(M) = \sum_{i=1}^M \Pi(i, M) \cdot P_L(N, i) \quad (8)$$

where $\Pi(i, M)$ is the probability of i packets out of M paths overlapping each other, which obeys the binomial distribution

$$\Pi(i, M) = \binom{M}{i} \rho^i (1 - \rho)^{M-i}. \quad (9)$$

From (7)–(9), we can see that the burst length does not have an impact on $\text{PLP}(M)$, which is suitable for traffic with variable burst length.

V. PERFORMANCE EVALUATION

In this section, OC-labeled and OCDM paths are compared. The parameters used in our numerical calculation are summarized in Table III.

A. PLP Characteristics of the OCDM Path

Fig. 8 illustrates the PLP property of the OCDM path. From (8), given a code length, it is evident that the PLP is determined by the number of connected paths and source utilization ρ .

Fig. 8(a) and (b) depicts how the number of connected paths affects the performance of the OCDM path with fixed source utilization. From the results shown, first, we can observe that the performance is actually degraded by the increase in the number of active users, due to the increase of MAI noise. Second, it is also evident that the OCDM path with a longer codeword outperforms that with a shorter codeword, which corresponds to what is described in [7]. Third, better performance

$$\hat{c}_i \approx \frac{\alpha b(1 - \rho)R_{\text{peak}} - B + \sqrt{[\alpha b(1 - \rho)R_{\text{peak}} - B]^2 + 4B\alpha b\rho(1 - \rho)R_{\text{peak}}}}{2\alpha b(1 - \rho)} \quad (5)$$

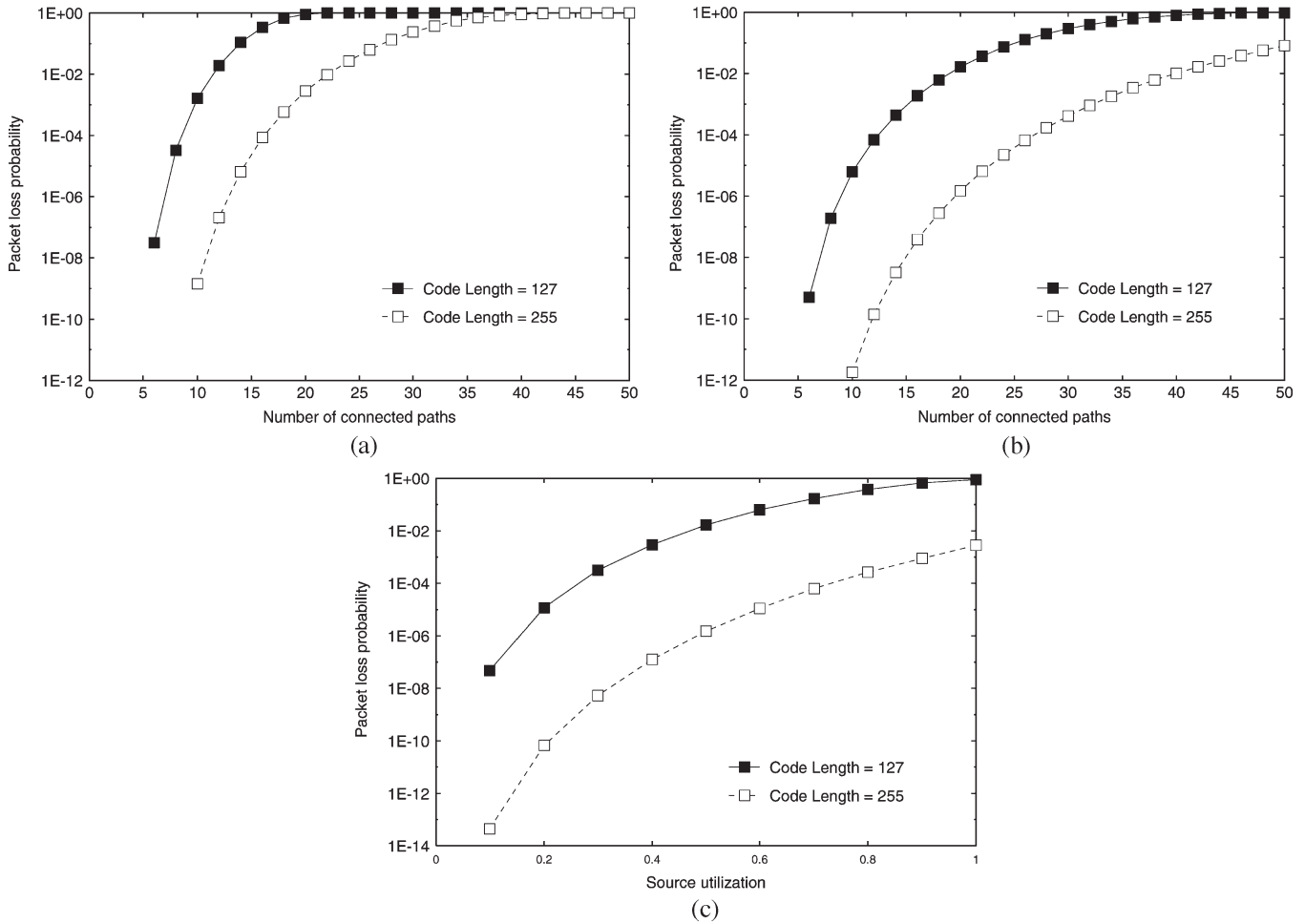


Fig. 8. PLP property of the OCDM path. Here, (a) and (b) are the cases with fixed source utilization with (a) $\rho = 1.0$ and (b) $\rho = 0.5$. (c) is the case with a fixed connected OCDM path N , where $N = 20$.

is attained in Fig. 8(b), as source utilization ρ decreases. Note that Fig. 8(a) can be regarded as the worst case in the OCDM path with $\rho = 1.0$, where the traffic is a continuous bit stream.

Based upon our proposed model, under a given number of connected OCDM paths, how source utilization ρ influences PLP is depicted in Fig. 8(c). From the result shown, packets tend to be lost more easily with higher source utilization, due to higher overlapping probability and BER.

B. Comparison Between OC-Labeled and OCDM Paths

Fig. 9 shows the PLP as a function of the maximum number of connected paths. Here, in the OC-labeled-path case, buffer sizes $B = 50$ and 100 are analyzed, while in the case of the OCDM-path case, code lengths $L = 127$ and 255 are studied.

In Fig. 9(a), under burst duration time $b = 0.0001$ s, the OC-labeled path with a buffer size $B = 100$ packets outperforms $B = 50$ packets, but the difference is reduced greatly with an increase of burst length, as is shown in Fig. 9(b) with $b = 0.001$ s. Both cases in the OC-labeled path perform better than the OCDM path with $L = 127$ under a maximum number of connected paths less than 16 and 26, respectively. In contrast, OCDM paths with $L = 255$ outperform both cases in the OC-labeled path with a maximum number of con-

nected paths larger than 12 and 16, respectively. In Fig. 9(b), with $b = 0.001$ s, the statistical-multiplexing effect in the OC-labeled path is small and leads to drastic performance degradation. On the contrary, the OCDM path will perform with the same behavior as Fig. 9(a), because of the independence of burst length. Consequently, we can conclude that a higher flexibility can be achieved in the OCDM path than in the OC-labeled path without suffering a severe performance degradation caused by long burst duration time, and it is considered to be one of the advantages of the OCDM path.

Fig. 10 depicts an intuitionist result to show how burst duration time b affects the performance of the OC-labeled and OCDM paths in the maximum number of connected paths. Here, we consider the case with $R_{\text{peak}} = 200$ Mb/s and $\text{PLP} = 10^{-8}$. As shown in Fig. 10, in the OC-labeled-path case, the number of connected paths decreases with the increase of burst duration time. Furthermore, a considerable multiplexing effect can be attained under a short burst duration time ($b < 0.001$ s). On the other hand, as the OCDM path is independent of burst duration time, the number of connected OCDM paths never changes. Fig. 10 also implies that source utilization ρ has an impact on the multiplexing effect under a short burst duration time in the OC-labeled-path case. The burst duration time b has a relatively slight influence with a heavier traffic load,

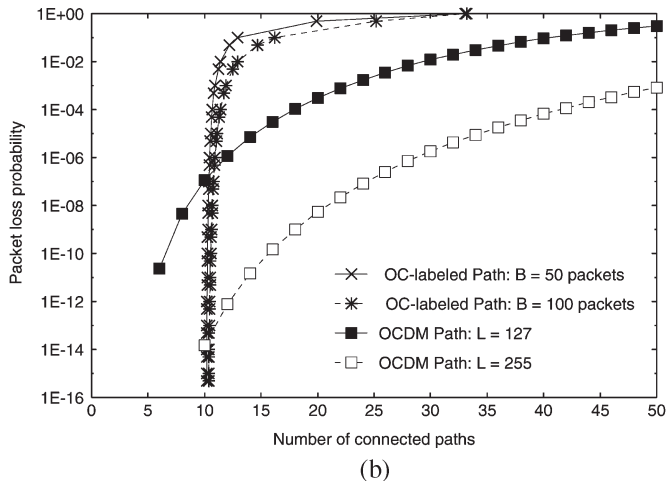
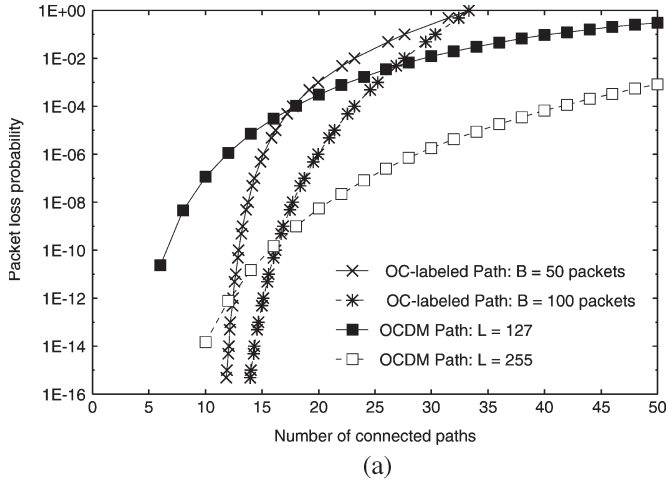


Fig. 9. Comparison between OC-labeled and OCDM paths with $R_{\text{peak}} = 1 \text{ Gb/s}$ and $\rho = 0.3$. (a) Burst duration time $b = 0.0001 \text{ s}$. (b) Burst duration time $b = 0.001 \text{ s}$.

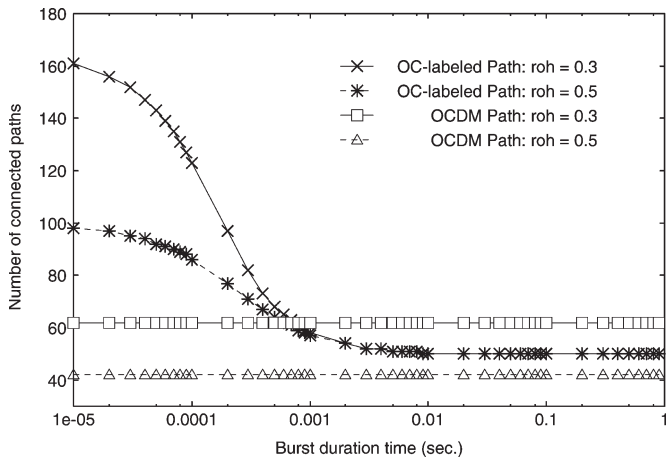


Fig. 10. Number of connected paths as a function of mean burst duration time with $R_{\text{peak}} = 200 \text{ Mb/s}$, $\text{PLP} = 10^{-8}$, code length $L = 1023$, and buffer size $B = 50$ packets.

e.g., $\rho = 0.5$, compared to $\rho = 0.3$, and the performance of both $\rho = 0.3$ and 0.5 become the same when $b > 0.001 \text{ s}$, which means that source utilization ρ has a small influence on the performance with a large burst duration time b . The same

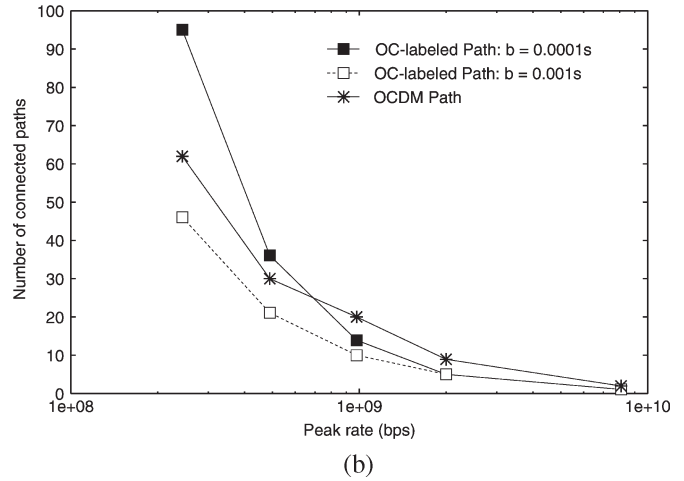
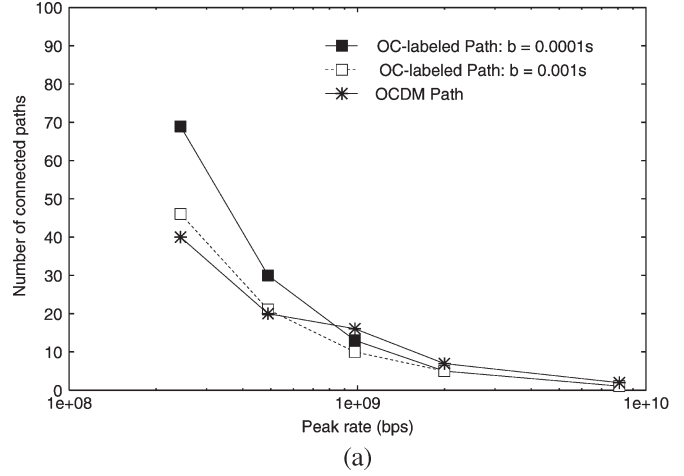


Fig. 11. Number of connected paths as a function of peak rate with chip duration time $\tau = 2 \text{ ps}$, buffer size $B = 50$, $\text{PLP} = 10^{-8}$, and (a) source utilization $\rho = 0.5$, and (b) source utilization $\rho = 0.3$.

tendency can be also attained with a different peak rate, which is not shown here.

In Fig. 11, the multiplexing effects of the proposed two approaches are compared in terms of peak rate R_{peak} . Different peak rates can be achieved with a fixed chip duration time τ and different code length. To perfectly avoid the overlapping of the correlation waveform sidelobes between the neighboring bits, chip duration time τ should be equal to $1/(2L \times R_{\text{peak}})$. Therefore, R_{peak} should be equal to $1/(2L \times \tau)$. Here, 31-, 127-, 255-, 511-, and 1023-chip-long codewords are analyzed. As the OCDM system with chip duration time $\tau < 2 \text{ ps}$ has been demonstrated successfully [31], we consider that $\tau = 2 \text{ ps}$ is also applicable in our simulation.

As shown in Fig. 11(a) and (b), first, in both cases of the OC-labeled and OCDM paths, the multiplexing effect tends to become small with a high peak rate, as a higher peak rate leads to faster buffer overflow in the OC-labeled path and shorter code length in the OCDM path. Second, in the OC-labeled path, the multiplexing-effect difference caused by burst duration time becomes small with high peak rates and source utilization ρ . Third, though the OCDM path is outperformed by the OC-labeled path with $b = 0.0001 \text{ s}$, even with $b = 0.001 \text{ s}$ in Fig. 11(a) with $\rho = 0.5$, under a peak rate smaller than 1 Gb/s ,

it outperforms the case of the OC-labeled path with $b = 0.001$ s in Fig. 11(b) and, moreover, achieves better performance than those in the OC-labeled path under a peak rate larger than 1 Gb/s in both Fig. 11(a) and (b).

VI. CONCLUSION

In this paper, a network architecture based upon the OC-based optical path is proposed, which is possibly considered as another type in the GMPLS network. The OC-labeled and OCDM paths are proposed to resolve the granularity problem inherent to a wavelength-routed network. Two OXCs with OC switching capability, called OC-label OXC and OCDM OXC, are presented to support the OC-based path switching. To achieve satisfactory performance in the OCDM path, a coherent OCDM system based upon the SSFBG using the gold code is employed. The SNR of different code lengths in such a system is also analyzed by the statistical approach.

In the OC-labeled-path case, statistical multiplexing is adopted and proved to be capable of evaluating the multiplexing effect with a different buffer-overflow probability, while in the OCDM-path case, the multiplexing capability in a single wavelength is investigated by using SNR based upon different levels of multiple-user interference. An approximate mathematical model for the OCDM path is proposed to estimate the PLP, which provides a simple but appropriate method in practical traffic engineering.

Through numerical results, we can conclude that using the OC-labeled and OCDM paths improves the efficiency of bandwidth utilization, and in addition to this, the maximum number of multiple optical paths that can be multiplexed in a single wavelength is capable of varying with different traffic characteristics, buffer size or code length, and different PLP. The numerical results also indicate that the OC-labeled path outperforms the OCDM path with short burst duration time in the multiplexing effect, while the OCDM-path case obtains higher flexibility in providing stable service than in the OC-labeled path, owing to its independence of burst duration time, and a simpler architecture can be obtained with nonbuffer operation.

ACKNOWLEDGMENT

The authors would like to thank Dr. X. Wang of the National Institute of Information and Communication Technology (NICT), Japan, for useful discussions and his valuable advice. S. Huang would like to thank Panasonic Scholarship, Inc., Japan.

REFERENCES

- [1] The Internet Engineering Task Force, "Generalized multi-protocol label switching (GMPLS) signaling functional description" *Request for Comments: RFC's 3471*. [Online]. Available: <http://www.ietf.org>
- [2] B. Wen and K. Sivalingam, "Routing, wavelength and time-slot assignment in time division multiplexed wavelength-routed optical WDM networks," in *Proc. IEEE Infocom*, New York, Jun. 2002, pp. 1442–1450.
- [3] K. Kitayama, "Code division multiplexing lightwave networks based upon optical code conversion," *IEEE J. Sel. Areas Commun.*, vol. 16, no. 7, pp. 1309–1319, Sep. 1998.
- [4] R. Guerin, H. Ahmadi, and M. Naghshien, "Equivalent capacity and its application to bandwidth allocation in high-speed networks," *IEEE J. Sel. Areas Commun.*, vol. 9, no. 7, pp. 968–981, Sep. 1991.
- [5] P. C. Teh, P. Petropoulos, M. Ibsen, and D. J. Richardson, "A comparative study of the performance of seven- and 63-chip optical code-division multiple-access encoders and decoders based on superstructured fiber Bragg gratings," *J. Lightw. Technol.*, vol. 19, no. 9, pp. 1352–1365, Sep. 2001.
- [6] P. C. Teh, M. Ibsen, L. B. Fu, J. H. Lee, Z. Yusoff, and D. J. Richardson, "A 16-channel OCDMA system (4 OCDM \times 4 WDM) based on 16-chip, 20 Gchip/s superstructure fiber Bragg gratings and DFB fiber laser transmitters," in *Proc. OFC Conf.*, Los Angeles, CA, 2002, pp. 600–601.
- [7] X. Wang, K. Matsushima, A. Nishiki, N. Wada, and K. Kitayama, "High reflectivity superstructured FBG for coherent optical code generation and recognition," *OSA Opt. Express*, vol. 12, no. 12, pp. 5457–5468, Nov. 2004.
- [8] Spohn and McDysan, *ATM: Theory and Applications*. New York: McGraw-Hill, 1994.
- [9] N. Wada and K. Kitayama, "A 10 Gb/s optical code division multiplexing using 8-Chip optical bipolar code and coherent detection," *J. Lightw. Technol.*, vol. 17, no. 10, pp. 1758–1765, Oct. 1999.
- [10] K. Kitayama, "Architectural considerations for photonic IP router based upon optical code correlation," *J. Lightw. Technol.*, vol. 18, no. 12, pp. 1834–1844, Dec. 2000.
- [11] R. S. Tucker and W. D. Zhong, "Photonic packet switching," *IEICE Trans. Commun.*, vol. E82-B, no. 2, pp. 254–264, Feb. 1999.
- [12] C. Guillemot *et al.*, "Transparent optical packet switching: The European ACTS KEPOS project approach," *J. Lightw. Technol.*, vol. 16, no. 12, pp. 2117–2134, Dec. 1998.
- [13] L. Dittman *et al.*, "The European IST project DAVID: A viable approach toward optical packet switching. Architecture and performance of AWG-based optical switching nodes for IP networks," *IEEE J. Sel. Areas Commun.*, vol. 21, no. 7, pp. 1026–1040, Sep. 2003.
- [14] D. K. Hunter, K. M. Guild, and J. D. Bainbridge, "WASPNET: A wavelength switched packet network," *IEEE Commun. Mag.*, vol. 37, no. 3, pp. 120–129, Mar. 1999.
- [15] D. K. Hunter, W. D. Cornwell, T. H. Gilfedder, A. Franzen, and I. Andonovic, "SLOB: A switch with large optical buffers for packet switching," *J. Lightw. Technol.*, vol. 16, no. 10, pp. 1725–1736, Oct. 1998.
- [16] A. Pattavina, "Architectures and performance of optical packet switching nodes for IP networks," *J. Lightw. Technol.*, vol. 23, no. 3, pp. 1023–1032, Mar. 2005.
- [17] L. Li, S. Scott, and J. Deogun, "A novel fiber delay line buffering architecture for optical packet switching," in *Proc. IEEE GLOBECOM*, New York, 2003, pp. 2809–2813.
- [18] V. Eramo and M. Listanti, "Packet loss in a bufferless optical WDM switch employing shared tunable wavelength converters," *J. Lightw. Technol.*, vol. 18, no. 12, pp. 1818–1833, Dec. 2000.
- [19] F.-S. Choa, X. Zhao, X. Yu, J. Lin, J. P. Zhang, Y. Gu, G. Ru, G. Zhang, L. Li, H. Xiang, H. Hadimioglu, and H. J. Chao, "An optical packet switch based on WDM technologies," *J. Lightw. Technol.*, vol. 23, no. 3, pp. 994–1014, Mar. 2005.
- [20] M. C. Chia, D. Hunter, I. Andonovic, P. Ball, I. Wright, S. Ferguson, K. Guild, and M. O'Mahony, "Packet loss and delay performance of feed-back and feed-forward arrayed-waveguide grating-based optical packet switches with WDM inputs-outputs," *J. Lightw. Technol.*, vol. 19, no. 9, pp. 1241–1253, Sep. 2001.
- [21] K. Kitayama and M. Murata, "Versatile optical code-based MPLS for circuit, burst, and packet switchings," *J. Lightw. Technol.*, vol. 21, no. 11, pp. 2753–2764, Nov. 2003.
- [22] H. Harai and M. Murata, "Prioritized buffer management in photonic packet switches for DiffServ assured forwarding," in *Proc. 6th Work. Conf. ONDM*, Torino, Italy, Feb. 2002, pp. 231–245.
- [23] D. D. Sampson, G. J. Pendock, and R. A. Griffin, "Photonic code-division multiple-access communications," *Fiber Integr. Opt.*, vol. 16, no. 2, pp. 126–157, Mar. 1997.
- [24] D. J. G. Mestdagh, *Fundamentals of Multiaccess Optical Fiber Networks*. Norwood, MA: Artech House, 1995.
- [25] P. R. Prucnal, M. A. Santoro, and T. R. Fan, "Spread spectrum fiber-optical local area network using optical processing," *J. Lightw. Technol.*, vol. LT-4, no. 5, pp. 547–554, May 1986.
- [26] J. A. Salehi and C. A. Brackett, "Code division multiple-access technique in optical fiber networks, part I: Fundamental principals and part II: Systems performance analysis," *IEEE Trans. Commun.*, vol. 37, no. 8, pp. 824–842, Aug. 1989.
- [27] X. Wang, K. Matsushima, A. Nishiki, N. Wada, F. Kubota, and K. Kitayama, "High-performance optical code generation and recognition

- using 511-chip 640-Gchip/s phase-shifted superstructured FBG," *Opt. Lett.*, vol. 30, no. 4, pp. 355–357, Feb. 2005.
- [28] Z. Jiang, D. S. Seo, S. D. Yang, D. E. Leaird, R. V. Roussev, C. Langrock, M. M. Fejer, and A. M. Weiner, "Four-user 10-Gb/s spectrally phase-coded O-CDMA system operating at 30 fJ/bit," *IEEE Photon. Technol. Lett.*, vol. 17, no. 3, pp. 705–707, Mar. 2005.
- [29] H. P. Sardesai and A. M. Weiner, "Nonlinear fibre-optic receiver for ultrashort pulse code division multiple access communications," *Electron. Lett.*, vol. 33, no. 7, pp. 610–611, Mar. 1997.
- [30] J. H. Lee, P. C. Teh, P. Petropoulos, M. Ibsen, and D. J. Richardson, "A grating-based OCDMA coding-decoding system incorporating a nonlinear optical loop mirror for improved code recognition and noise reduction," *J. Lightw. Technol.*, vol. 20, no. 1, pp. 36–46, Jan. 2002.
- [31] X. Wang, T. Hamanaka, N. Wada, and K. Kitayama, "Dispersion-flattened-fiber based optical threshold for multiple-access-interference suppression in OCDMA system," *OSA Opt. Express*, vol. 13, no. 14, pp. 5499–5505, Jul. 2005.
- [32] A. A. Shaar and P. A. Davies, "Prime sequences: Quasi-optimal sequences for Or channel code division multiplexing," *Electron. Lett.*, vol. 19, no. 21, pp. 888–889, Oct. 1983.
- [33] F. R. K. Chung, J. A. Salehi, and V. K. Wei, "Optical orthogonal codes: Design, analysis, and applications," *IEEE Trans. Inf. Theory*, vol. 35, no. 3, pp. 595–604, May 1989.
- [34] S. Tamura, S. Nakano, and K. Akazaki, "Optical code-multiplex transmission by gold sequences," *J. Lightw. Technol.*, vol. LT-3, no. 1, pp. 121–127, Feb. 1985.
- [35] X. Wang and K. Kitayama, "Analysis of beat noise in coherent and incoherent time-spreading OCDMA," *J. Lightw. Technol.*, vol. 22, no. 10, pp. 2226–2235, Oct. 2004.
- [36] E. K. H. Ng and E. H. Sargent, "Optimum threshold detection in real-time scalable high-speed multi-wavelength optical code-division multiple-access LANs," *IEEE Trans. Commun.*, vol. 50, no. 5, pp. 778–784, May 2002.



Shaowei Huang (S'06) received the B.E. degree from the Department of Electrical and Electronics Engineering, Nankai University, Tianjin, China, in 2002 and the M.E. degree from the Department of Electrical, Electronics, and Information Engineering, Osaka University, Osaka, Japan, in 2006. He is currently working toward the Ph.D. degree with the Department of Electrical, Electronics, and Information Engineering, Osaka University, concentrating on optical communication networks.

Mr. Huang is a Student Member of the Institute of Electrical, Information, and Communication Engineers (IEICE) of Japan.



Ken-ichi Baba received the B.E., M.E., and D. E., degrees in information and computer sciences from Osaka University, Osaka, Japan, in 1990, 1992, and 1995, respectively.

After quitting the doctoral course in 1992, he was a Research Associate with the Education Center for Information Processing, Osaka University, until 1997. In 1997, he was an Assistant Professor with Electronic and Photonic Systems Engineering, Kochi University of Technology, Kochi, Japan. He has been an Associate Professor with Cybermedia Center (then Computation Center), Osaka University, since December 1998. His research interests include the broadband communication network, the computer communication network, and photonic network systems.



Masayuki Murata (M'89) received the M.E. and D.E. degrees in information and computer sciences from Osaka University, Osaka, Japan, in 1984 and 1988, respectively.

In April 1984, he joined Tokyo Research Laboratory, IBM Japan, as a Researcher. In 1987, he moved to Osaka University. Currently, he is a Professor in the Graduate School of Information Science and Technology, Osaka University. He has more than 400 papers in international and domestic journals and conferences. His research interests include computer communication network architecture and performance modeling and evaluation.

Dr. Murata is a member of the Association for Company Machinery (ACM), The Internet Society, the Institute of Electrical, Information, and Communication Engineers (IEICE), and the Information Processing Society of Japan (IPSI).



Ken-ichi Kitayama (S'75–M'76–SM'89–F'03) received the B.E., M.E., and Dr.Eng. degrees in communication engineering from Osaka University, Suita, Japan, in 1974, 1976, and 1981, respectively.

In 1976, he joined the NTT Electrical Communication Laboratory. During 1982–1983, he was a Research Fellow with the University of California, Berkeley. In 1995, he joined the Communications Research Laboratory (now the National Institute of Information and Communications Technology, NiCT), Tokyo, Japan. Since 1999, he has been a Professor with the Department of Electrical, Electronic, and Information Engineering, Graduate School of Engineering, Osaka University. He has published more than 200 papers in refereed journals, written two book chapters, and translated one book. He is also the holder of more than 30 patents. His research interests include photonic networks, optical signal processing, optical-code-division multiple-access-based fiber-to-the-home systems, and radio-on-fiber communications.

Prof. Kitayama was a recipient of the 1980 Young Engineer Award from the Institute of Electronic and Communication Engineers of Japan, the 1985 Paper Award of Optics from the Japan Society of Applied Physics, and the 2004 Achievement Award from the Institute of Electronics, Information, and Communication Engineers (IEICE) of Japan. He is currently an Associate Editor of the IEEE PHOTONICS TECHNOLOGY LETTERS and the IEEE TRANSACTIONS ON COMMUNICATIONS, *Optical Switching, and Networking*. He is a Fellow of the IEICE of Japan.